Vibronic Spectroscopy of Single C_{60} Molecules and Monolayers with the STM†

Nilay A. Pradhan, Ning Liu, and Wilson Ho*

Department of Physics and Astronomy and Department of Chemistry, University of California, Irvine, California 92697-4575

Received: October 14, 2004; In Final Form: November 12, 2004

A scanning tunneling microscope is used to study the differential conductance (dI/dV) of single C_{60} molecules in isolation and in monolayers adsorbed on NiAl(110) and on an ultrathin alumina film grown on the NiAl-(110) surface. On the oxide layer, the electronic bands in the dI/dV spectra display a series of equally spaced features, attributed to the vibronic states of the molecules, which are absent when the molecules are adsorbed on the metal. A comparison between the molecular spectra measured on the oxide film reveals the effect of adsorption temperature and geometry, as well as intermolecular interactions on the vibronic features.

Introduction

In recent years, research on the transmission of electrons through molecules and molecular interfaces has gathered intense following, partly because of its importance in the emerging field of molecular electronics.[1] These processes endorse the view of molecules as conductors and heighten the importance of current−voltage characteristics of molecular junctions.[1−3] Furthermore, the transient electron flow can couple to molecular excitations such as librations and intramolecular as well as intermolecular vibrations and reveal additional details about the electron-transfer processes at these junctions.[4] One of the most widely studied areas in this field has been electron−phonon coupling in doped fullerenes, especially since the discovery of superconductivity in A_3C_{60} (A = K, Rb, Cs)[5] where the general consensus is that the intramolecular H_g modes are the most likely contributors to the pairing mechanism.[6] Recent observations of satellite features in the $I-V$ characteristics of fullerene-based field effect transistor (FET) devices have renewed interest in the study of the coupling between electron current and molecular vibration.[7,8]

In the FET experiments, the molecular environment is not precisely known. The dependence of characteristic features in the electronic spectra on the orientation of the molecule(s) and their immediate surroundings can yield valuable knowledge that is likely to play an important role in future applications. Such a requirement calls for techniques that can discern spatial as well as spectroscopic detail with submolecular precision. The scanning tunneling microscope (STM), with its ability to provide resolution at the atomic scale, is ideally suited to probe such systems.[9] Indeed, vibrational analysis with single bond sensitivity has been demonstrated by STM-based inelastic electron tunneling spectroscopy (STM-IETS).[10] In this technique, one measures the change in conductance at the threshold of a vibrational mode energy in a single molecule adsorbed on a metal surface. However, this necessitates that the substrate conducts well near the Fermi level, since the vibrational energies are within a fraction of an electronvolt about the Fermi energy.

In this article, we address the problem of vibrational analysis on a substrate that conducts poorly at low sample bias. We measure the STM current and differential conductance through single C_{60} molecules adsorbed on an ultrathin Al_2O_3 film grown on NiAl(110). The oxide layer separates the molecules from the surface of the metal, extending the lifetime of the transient excited state. As a result of this, vibrational features are seen in the differential conductance (dI/dV) spectra of these molecules because of resonant tunneling into their vibronic states. Such features are absent in the spectra of molecules adsorbed on the metal surface. Measurements over isolated molecules (reported in a previously published work)[11] are compared to those performed over molecules embedded in monolayers, newly reported here. Our results reveal the dependence of dI/dV features on the molecular adsorption geometry and environment.

Experimental Methods

The experiments were performed with a homemade, variable-temperature STM whose construction has been detailed elsewhere.[12] The design of the microscope allows dosing of desired species on a substrate from room temperature (RT) down to 11 K. The experiments were performed under ultrahigh vacuum with pressure lower than 3×10^{-11} Torr. The dI/dV as well as the d^2I/dV^2 spectra were recorded through lock-in detection of the ac tunneling current achieved by modulating the sample bias (10 mV, 250 Hz) while keeping the feedback loop open. The NiAl(110) crystal was prepared by successive cycles of Ne^+ sputtering and annealing up to 1300 K. The clean surface was then exposed to 330 L of O_2 (1 L = 1×10^{-6} Torr exposure for 1 s) at 750 K and subsequently annealed to 1200 K to yield a crystalline ultrathin (∼5.2 Å thick)[13] alumina film covering nearly 50−60% of the NiAl(110) surface. The C_{60} (Aldrich, 99.9% purity) was evaporated out of an alumina crucible with the sample kept at room temperature to obtain monolayer thick islands and at 11 K to obtain isolated molecules. The tips were fabricated from polycrystalline Ag and were subjected to Ne^+ sputtering and annealing. All topographic imaging and spectroscopic measurements were carried out at 11 K.

Results and Discussion

Figure 1 shows the four main topographic areas of interest consisting of a combination of C_{60} molecules dosed at RT and 11 K on the metal and oxide substrates. Typical dI/dV spectra of each spectroscopically distinct species and surface are

† Part of the special issue "George W. Flynn Festschrift".

* Corresponding author. E-mail: wilsonho@uci.edu.

10.1021/jp045289b CCC: $30.25
Published on Web 02/12/2005

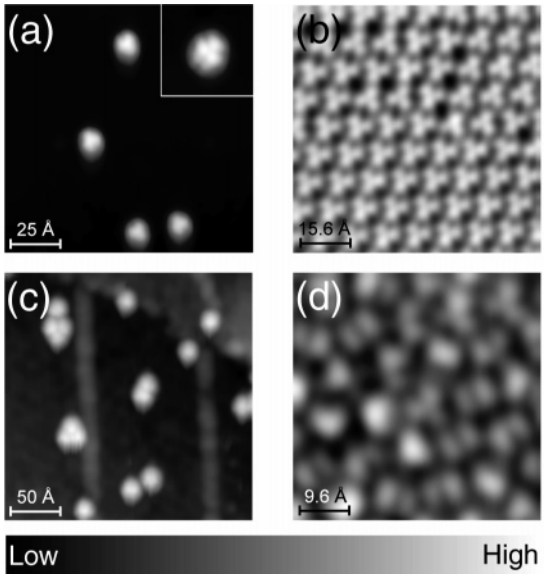

Figure 1. The four principal environments imaged at 11 K. The topography shows various molecular orientations. The scale is indicated in each image. (a) Topographic image of a NiAl(110) surface dosed with C_{60} at 11 K, with the tunneling current at 15 pA and sample bias voltage at 2.5 V. The topographic features are detailed in the inset. (b) A monolayer coverage of C_{60} on NiAl(110) with the fullerene dosed at RT and cooled prior to imaging. All molecules appear to be adsorbed with the hexagon facing up. The tunneling conditions are 0.1 nA and 2.5 V. (c) C_{60} molecules dosed at 11 K on an ultrathin Al_2O_3 film prepared on NiAl(110) and imaged with the tunneling gap fixed at 15 pA and 2.5 V. (d) An overlayer formed by dosing C_{60} at RT onto Al_2O_3 on NiAl(110), imaged at the conditions 0.1 nA and 2.5 V.

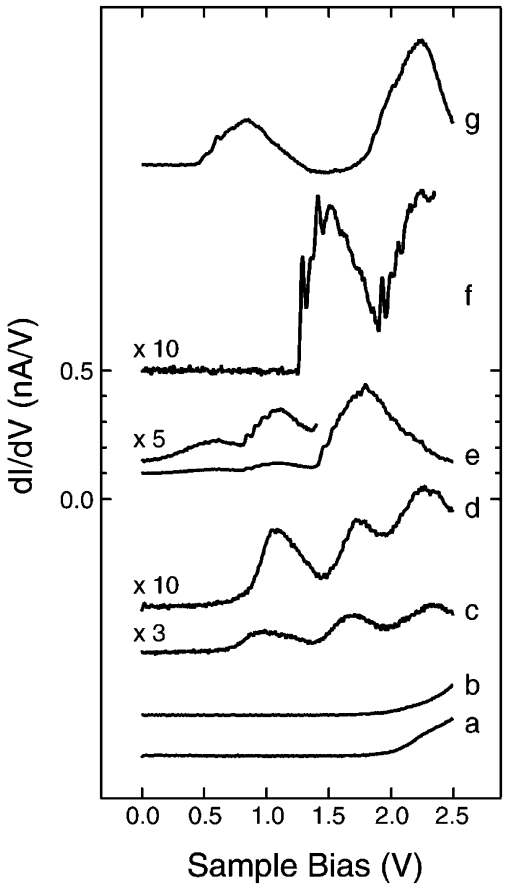

Figure 2. dI/dV spectra of the different environments. (a) Spectrum of the bare NiAl(110) surface, recorded with the tunneling gap set at 0.1 nA and 2.75 V. (b) Oxide terrace on NiAl(110) with gap set at 0.1 nA and 2.75 V. (c) C_{60} island on metal, measured directly above the molecule, with gap set at 0.1 nA and 2.75 V. (d) Isolated C_{60} molecule on metal, with the gap fixed at 50 pA and 2.5 V. (e) Single C_{60} molecule on oxide, exhibiting three bands in the spectrum, gap set at 0.2 nA and 2.25 V. (f) Single C_{60} molecule on oxide with two bands in the spectrum, gap set at 50 pA and 2.4 V. (g) C_{60} island on oxide, gap set at 0.1 nA and 2.0 V. Each spectrum was measured in the bias range 0−2.5 V, (except (f), whose range is 0−2.35 V) and averaged over four passes (at the rate of 50 s/V, i.e., 4 min 10 s per pass). The traces are offset and scaled as needed for clarity.

displayed in Figure 2. The C_{60} molecules can be clearly detected from the STM topographic images on both clean and oxidized areas of the surface after in situ evaporation at 11 K. On the metal, C_{60} molecules are typically isolated and assume the shape of three-lobed protrusions, indicating that the molecules adsorb with a hexagon parallel to the surface, as can be seen from Figure 1a. The topographical image and spectrum of such a molecule, measured at its center, is shown in Figure 2d and detailed in Figure 3a−d. No fine features are revealed in these spectra, as exemplified by the electronic state around 1.0 V in the differential conductance dI/dV shown in Figure 3b−d.

The molecules interact only weakly with the oxide, leading to a greater variety of adsorption geometries (see Figure 1c). These differences in topography are reflected in the spectra as well. However, the spectra from the isolated C_{60} molecules can be broadly classified into two groups. The first group consists of dI/dV spectra containing two bands in the range 0 to 2.5 V (see Figure 2f), as we see in the case of the molecule indicated by the white arrow in Figure 4a. In this group, the onset of the first band falls between 0.3 and 1.2 V (here at 1.1 V). The second group of spectra, exemplified by the ones in Figures 2e and 4f−j, shows three distinct bands in the interval from 0 to 2.5 V. In this case, the first band commences between 0 and 0.3 V.

These differences can be understood if we take into account the locally irregular nature of the oxide film itself. Given the complex structure of the alumina film described in recent literature,[13,14] the local inhomogeneities within the film can influence the orientation adopted by the molecules upon adsorption and alter the electronic configuration of the molecule. The unit cell of the oxide is large compared to that of the underlying metal. However, it is not possible to atomically resolve the oxide surface at the same tunneling conditions used to image the molecules, making the determination of the exact adsorption site difficult. It is also known from previous studies of Al_2O_3 films on NiAl(110)[15] that the oxide layer can be a host to charge traps arising from unsaturated electronic states associated with structural defects on the surface. This charge may be partially transferred to the molecule in local contact with the defect state, thus altering its electronic configuration and hence its dI/dV spectrum.

As remarked above, the spectra recorded on the metal surface are smooth. However, spectra from the alumina-supported molecules display equally spaced features. These distinctive characteristics are further clarified in the d^2I/dV^2 spectra (see Figure 4d,i). We attribute them to vibronic states of the C_{60}^- anion, and their observation on molecules adsorbed on the oxide layer is due to extended lifetime of the transient charged state of the molecule.[11,16] In Figure 4d, we observe two vibronic progressions with the same spacing for the C_{60} molecules with the two-band electronic structure. In Figure 4i, we notice three vibronic series for the C_{60} with the three-band electronic structure. The first one has a spacing different from the other two. The energies of the peaks in Figure 4c,h are plotted as a function of their positions in the progressions in Figure 4e,j, respectively. The slope, which represents the mean separation

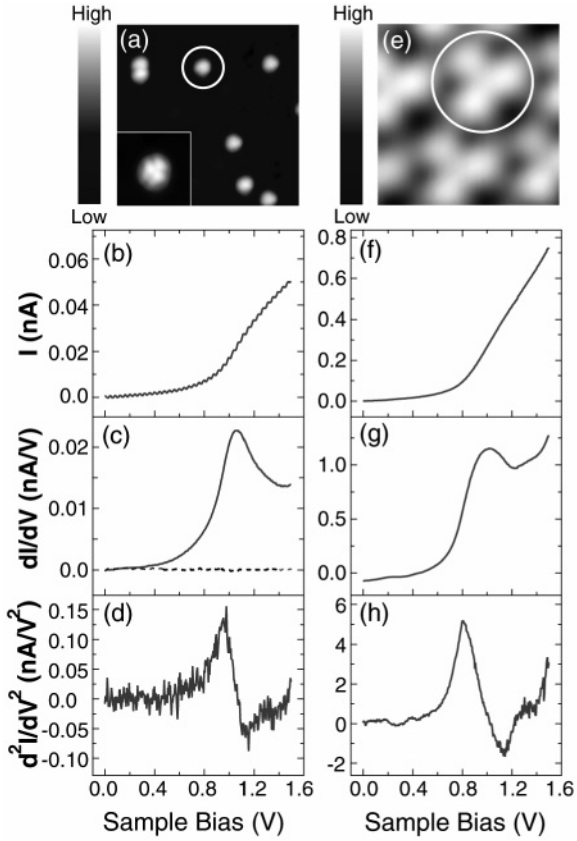

Figure 3. (a) STM topographic image recorded at 15 pA and 2.5 V (175 Å × 175 Å) of C_{60} molecules dosed at 11 K on the bare NiAl(110) surface (details shown in inset). (b)−(d) Simultaneously acquired spectra of tunneling current I, dI/dV, and d^2I/dV^2 vs sample bias V, measured over the C_{60} molecule indicated by the white circle in (a), averaged over 33 passes (2 min 40 s per pass; one pass indicates both forward and backward sweeps through the bias range). The tunneling gap was fixed with 45 pA and 1.5 V. A background spectrum of the NiAl(110) surface recorded with tunneling gap set at 75 pA and 2.75 V is shown as a dotted line in the dI/dV spectrum. (e) Image (20 Å × 20 Å) taken over a C_{60} monolayer on metal (dosed at room temperature) at 0.1 nA and 2.5 V. (f)−(h) Corresponding spectra recorded over a molecule circled in (e), averaged 43 times (2min 40 s each pass) with the gap set at 0.75 nA and 1.5 V.

between the peaks, is observed to be 65 ± 4 meV for the two-band C_{60} as well as for the second and third bands of the three-band C_{60}. This energy is ascribed to the radial, nondegenerate $A_g(\omega_1)$ vibrational mode of the neutral molecule.[6] The slope of the first vibronic progression of the three-band C_{60} molecule is 94 ± 3 meV, which is close to the Raman active $H_g(\omega_4)$ mode in neutral C_{60}. We have considered the H_g and A_g modes out of the many possibilities because of the known strength of electron−phonon coupling of these modes.[6]

The presence of inhomogeneities on the oxide surface, for example, defects, domain boundaries, or the oxide-metal step boundaries, further add to this topographical and spectroscopic diversity, as can be visualized from Figure 1c. However, only the molecules that are placed on the oxide terraces exhibit vibronic spectra. Vibronic progressions are not resolved from the spectra of molecules close to the domain boundaries or the oxide-metal step boundaries.

At this point, it must be mentioned that the spacings observed between the features in the progressions should be greater than the actual vibrational energies because of a finite voltage drop across the Al_2O_3 film. However, the correct renormalization of the spacings is only possible after the local dielectric properties of the oxide layer are known accurately, and therefore we can

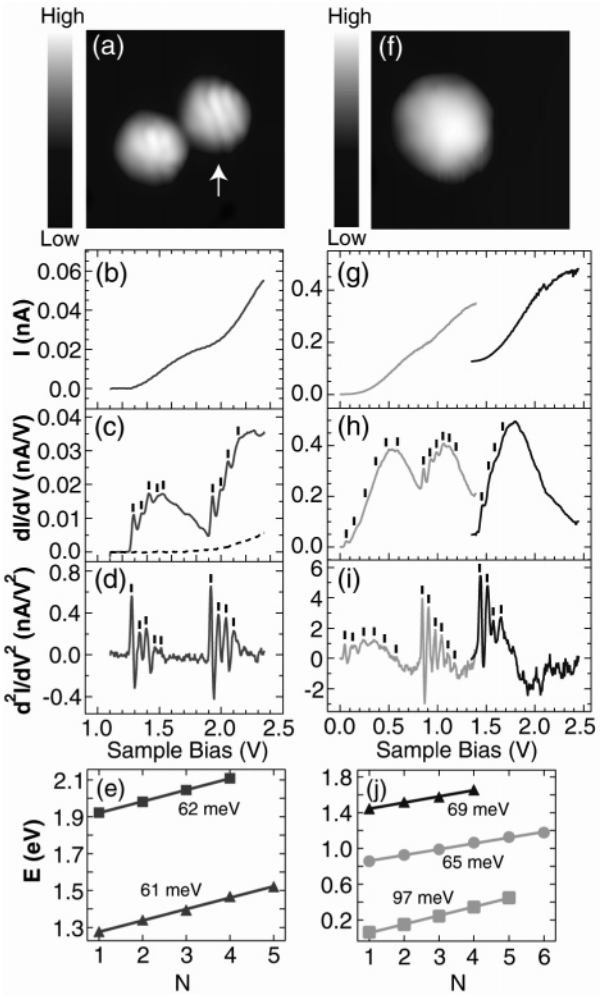

Figure 4. (a), (f) STM topographic images of C_{60} molecules dosed onto Al_2O_3 on NiAl(110) at 11 K. Image (a) measures 62.5 Å × 62.5 Å and was obtained at 15 pA and 2.25 V, whereas (f) is 45 Å × 45 Å and scanned at 0.1 nA and 2.0 V. (b)−(d) Spectra of tunneling current I, dI/dV, and d^2I/dV^2 vs sample bias V measured with the tunneling gap set at 45 pA and 2.3 V over the C_{60} molecule indicated by the white arrow in (a), averaged over 24 passes (2 min each pass). For comparison, the dotted line is a dI/dV spectrum over the oxide film with the gap set at 75 pA and 2.75 V. (g)−(i) Spectra recorded over the molecule in (f). A portion of the spectrum between 0 and 1.4 V was obtained with the tunneling gap set at 0.2 nA and 0.9 V and was averaged over 30 passes (2 min 20 s per pass). Between 1.35 and 2.45 V, the spectrum was measured with the gap set at 0.2 nA and 2.24 V and averaged over 53 passes (2 min per pass). In (c), (d), (h), and (i), the progressions are marked with vertical lines. (e), (j) Plots of the peak energy E vs peak number N for the progressions in spectra (c), (d) and (h), (i), respectively. The slope of each linear fit gives the mean separation of the peaks in the progression and, hence, the energy of the vibrational mode.

only estimate that the actual energy of the modes is a few percent lower than the observed peak separation. In addition, we must reiterate the fact that these features are representative of the excitations of a transient negative ion, and hence an assignment based on the symmetries and energies of an isolated neutral molecule is an approximation.

To exemplify the local nature of the tunneling process, we have acquired spectroscopic maps at loci within the same isolated molecule, as illustrated in Figure 5a−d. The dI/dV spectra exhibit differences among themselves and thus reveal a local dependence, presumably due to the distribution of the electronic orbitals. The vibronic features, well distinguished in

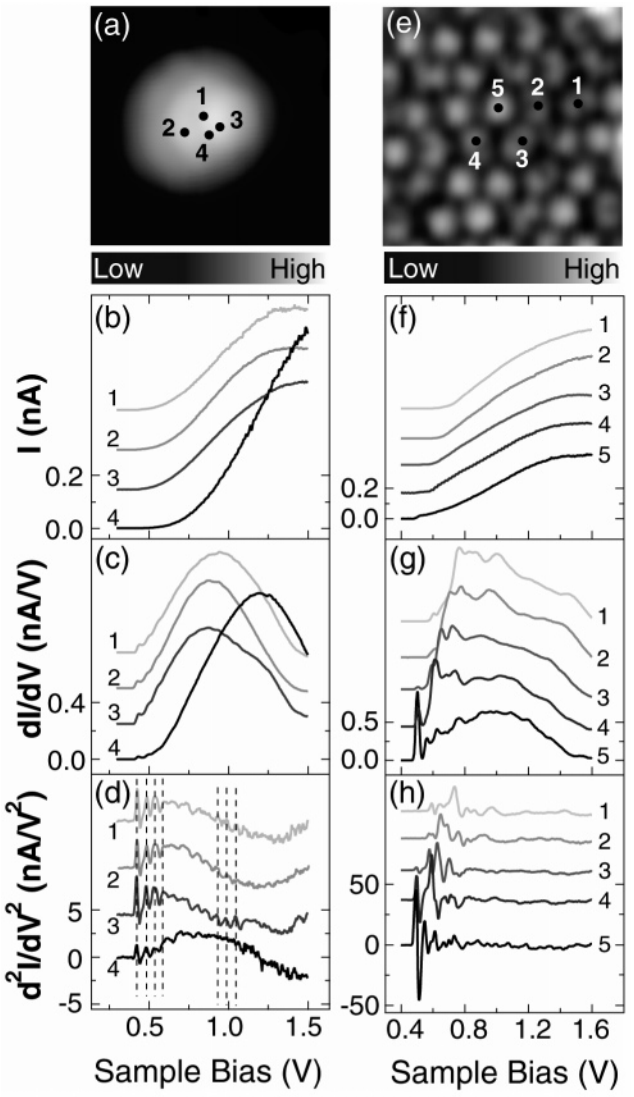

Figure 5. Topographic images and spectroscopic mapping recorded at 11 K over an isolated C_{60} molecule (a−d) and over neighboring molecules in a monolayer (e−h) on Al_2O_3/NiAl(110). The traces are offset for clarity. Image (a) is 38 Å × 38 Å and scanned with the tunneling parameters 0.1 nA and 2.0 V. (b)−(d) I, dI/dV, and d^2I/dV^2 spectra measured as functions of the sample bias V at the points indicated in (a). The tip−sample separation was kept constant and set at 0.25 nA and 1.0 V. Each trace was averaged over 25 passes (2 min 30 s per pass). (f)−(h) Corresponding spectra over the five molecules indicated in (e), with the tunneling gap set at 0.25 nA and 1.0 V and averaged over 30 passes (2 min per pass).

the d^2I/dV^2 spectra are, however, nearly identical in their positions, as indicated by the dashed lines in Figure 5d.

The temperature at which the molecules are dosed affects their adsorption geometry. Molecules adsorbed at 11 K have poor diffusion after they land on the surface of the metal as well as the oxide layer. On the other hand, when dosed on the NiAl(110) surface at room temperature, C_{60} is observed to form islands of sizes varying from 10 to 50 molecules that preferentially align along the direction of the Ni rows. Because of the lattice mismatch between the fullerenes and the substrate, they form an imperfect hexagonal structure, with each molecule seen as a three-lobed protrusion (see Figure 1b). In contrast, on the Al_2O_3 film, the fullerene molecules dosed at RT form nearly perfect hexagonal layers (Figure 1d), with almost the same lattice constant as that in bulk fullerite.[6] Unlike those adsorbed on the metal, these molecules do not share the same orientation. Instead, they adopt one of three possible geometries randomly dispersed throughout the monolayer: a round or donut (pentagon on top), a two-lobed species (double bond on top), or a three-lobed version (hexagon on top).[17]

The image of a typical molecule adsorbed within a monolayer on the bare NiAl(110) is shown and indicated by a white circle in Figure 3e. The spectrum of the molecule is displayed in Figure 2c. In the bias range between 0 and 1.6 V, shown in Figure 3f−h, a single peak is observed at 1.1 V. As in the case of single molecules adsorbed on NiAl(110) at low temperature, no vibronic progressions are detected in the dI/dV spectra. In contrast, for the C_{60} layer adsorbed on alumina, the spectra are nearly identical, displaying two bands in the bias range from 0 to 2.5 V (see Figure 2g). The onset of the first band is around 0.5 V (with very small variations), and the second band commences between 1.7 and 1.8 V. However, no discernible progressions are observed in the second band. Hence from now on, we shall elaborate on the details found within the first band only.

The topographic and spectroscopic details of the principal molecular orientations in C_{60} islands grown on the Al_2O_3 film are shown in Figure 6.[18] In the case of a round molecule, like the one circled in Figure 6a, the dI/dV spectrum displays two vibronic progressions, which are marked by the asterisks and vertical lines in Figure 6c and further clarified in the d^2I/dV^2 spectrum in Figure 6d. The energies of the peaks in Figure 6c are plotted in Figure 6e as a function of their position within the sequence. The two series have almost identical slope. The peaks in the progression marked by asterisks are spaced by an interval of nearly 150 meV, whereas the progression marked by vertical lines has a slope of 149 meV. These values correspond most closely to the energy of the intramolecular Raman active $H_g(\omega_6)$ mode of the neutral molecule.[6] A similar analysis performed on a two-lobed molecule depicted in Figure 6f reveals that the dI/dV spectra shown in Figure 6h also have two series of peaks. The d^2I/dV^2 spectrum in Figure 6i is again helpful in precisely resolving these peaks, which are plotted in Figure 6j. Two series with the slopes 138 and 140 meV are seen. These values coincide most nearly with the energy of the $H_g(\omega_5)$ mode of neutral C_{60}.[6] For both the round and the two-lobed species, the two series are separated by an interval of 56 ± 2 meV, which is close to the energy of the $H_g(\omega_2)$ mode. However, for the three-lobed molecule shown in Figure 6k, only one progression is observed. The peak positions of these features are plotted in Figure 6o. The spacing is 54 meV, that is, close to the energy of the $H_g(\omega_2)$ mode.

The presence of two progressions in the spectra of the round and the two-lobed molecules raises several questions. It is possible that the two different progressions are observed because of a partial lifting of the LUMO degeneracy.[19] However, previous works have shown that, for the C_{60}^- anion, the difference in energy between the previously degenerate LUMO derived levels is 3.75 and 9.4 meV,[20−22] thus precluding this possibility. Furthermore, given the relative uniformity of the C_{60} electronic spectra, this degeneracy lifting is expected to affect all orientations of the C_{60}, contrary to our observations. The other possibility is that the two series correspond to a progression of vibronic progressions involving an $H_g(\omega_6)$ [or $H_g(\omega_5)$] mode and another mode, such as the $H_g(\omega_2)$. This progression of progressions is a property of all nonlinear polyatomic molecules where each level of the first progression (ν_1) is an initial state of the progression of the second vibration (ν_2). This is schematically illustrated in Figure 7, where the successive features in the dI/dV spectrum in Figure 6c are

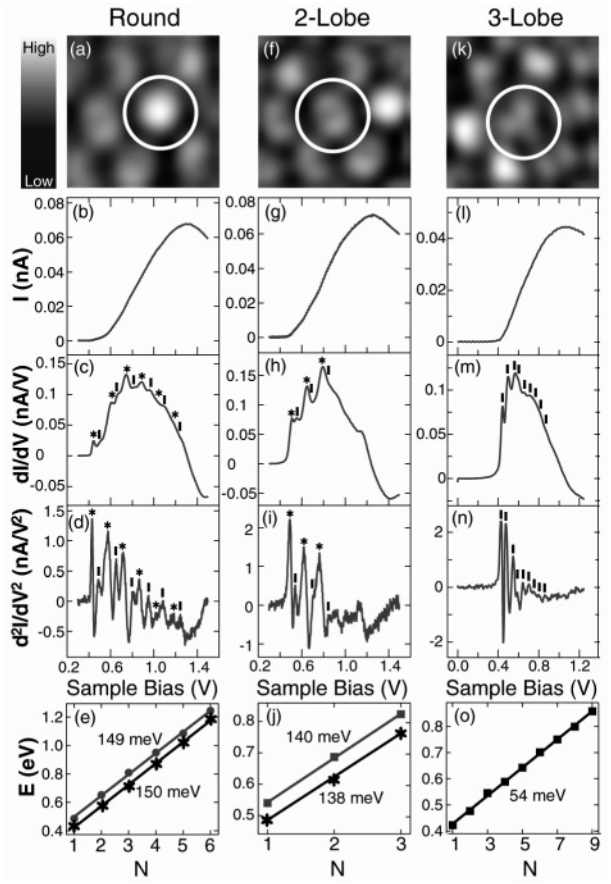

Figure 6. STM topography and spectroscopy over a monolayer of C_{60} on Al_2O_3/NiAl(110) at 11 K; molecules initially deposited at room temperature. (a), (f), (k) 25 Å × 25 Å topographic images scanned at 15 pA and 1.65 V. (b)−(d) Spectra of tunneling current I, dI/dV, and d^2I/dV^2 vs sample bias V measured over the C_{60} molecule indicated by the white circle in (a), averaged over 25 passes (2 min per pass). The set point for the tunneling gap was 45 pA and 1.65 V. (g)−(i) Similar spectra obtained over the two-lobed molecule indicated by a white circle in (f), with tunneling gap fixed at 45 pA and 1.65 V and averaged over 10 passes (2 min per pass). (l)−(n) STS spectra for the three-lobed molecule circled in (k). The measurements were performed with the gap set at 40 pA and 1.0 V and averaged over 38 passes (2 min per pass). (e), (j), (o) Plots of the peak energy E vs peak number N for the progressions in the spectra marked by asterisks (*) and vertical lines (|) in (c) and (d), (h) and (i), and (m) and (n), respectively. The slope of each trace gives the mean separation of the peaks in the progressions and, hence, the energy of the vibrational mode.

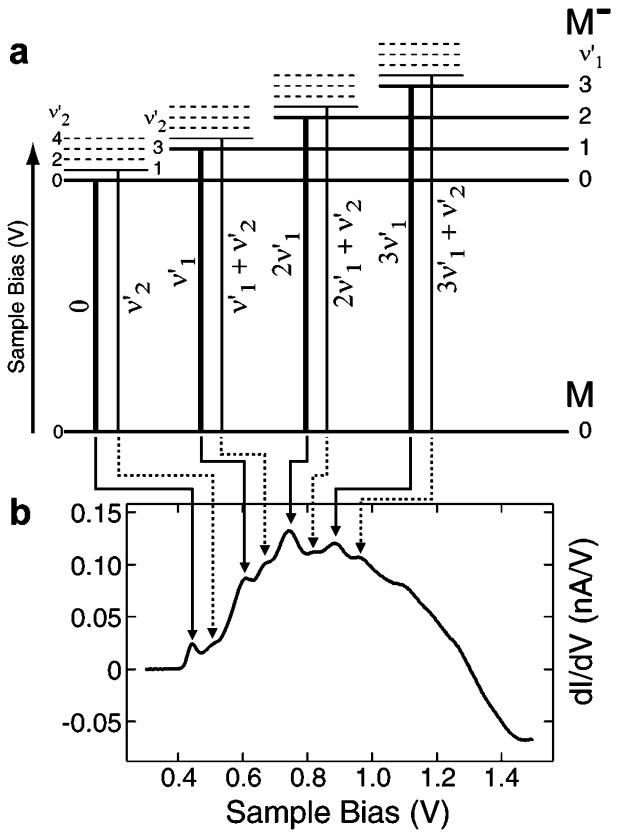

Figure 7. Schematic diagram of the "progression of progressions" in the case of the round molecule (Figure 6a−e). (a) The energy levels represent the molecular states before and after the tunneling of an electron into the molecule. The lower level (only the ground state is shown) represents the neutral molecule (M), whereas the transient negative ion (M^-) is represented by the upper levels. Transitions from the ground level to levels of the higher energy (ν_1') mode are indicated by the thick lines, whereas those involving the lower energy (ν_2') mode are indicated by the thin lines. (b) The assignment of the transitions to the levels of ν_1' and ν_2' modes in (a) to the spectral features of the dI/dV curve of the round molecule is indicated by the solid and the dotted lines, respectively. A similar scheme is expected to hold for the two-lobed molecule.

assigned to the first (ν_1') and the second (ν_2') modes of the anion M^-. At low temperature, only the transitions closest to the lowest levels are likely to be observed.[23]

For the case of the three-lobed molecule, we observe the $H_g(\omega_2)$ mode, as was detected by STM-IETS on similarly oriented C_{60} molecules on Ag(110).[24] Because of the relatively weak interaction of the fullerene overlayer with the oxide film and their moderate van der Waals interactions with each other, the vibrational symmetry is only slightly perturbed, resulting in a $H_g(\omega_2)$ component in all the vibronic spectra. The presence of the other partner in the "progression of progressions", namely the $H_g(\omega_6)$ and $H_g(\omega_5)$ modes for the round and two-lobed molecules, respectively, may depend on the specific adsorption geometry of the molecule as well as its neighbors and the underlying oxide film. As in the case of isolated molecules, the coupling of the tunneling electrons with the intramolecular vibrational modes depends on the symmetry of the mode as well as the symmetry of the molecular electronic state reflected by the adsorption geometry. These factors also influence the Franck−Condon factors of the corresponding vibronic transitions, which in turn determine the strength of a particular mode in the resultant dI/dV spectrum.

The effect of the molecular environment on its spectroscopic features is demonstrated in Figure 5e−h. Here, we perform a dI/dV mapping on a set of two-lobed molecules (except for molecule 5, which is round). The spectra over the molecules display a few identical features, although some features are unique to each molecule. On the basis of the mapping on the isolated molecule in Figure 5a−d, we expect that the d^2I/dV^2 spectra of these molecules will be identical (again, except for molecule 5). However, we can see from Figure 5h that this is not the case. The differences in the molecular spectra are a reflection of the molecule's interactions with the substrate as well as with its neighbors. If the six nearest neighbors of each two-lobed C_{60} are taken into account, then each molecule is in a unique environment. Furthermore, it is seen from Figure 5g,h that the molecules placed next to each other have more common features in their spectra than similarly oriented molecules further away. Thus, the spectra of the isolated molecules are influenced by their local interaction with the substrate, whereas the molecules in monolayers interact locally with the substrate as well as with their neighbors. Although the modes corresponding to the intermolecular interactions are not observed (possibly

because of the limited resolution of the instrument[25]), they contribute to the actual line shape.

Although the experimental methods described above allow us to determine the vibronic structure with submolecular precision, they leave a few questions unanswered. For instance, it is impossible to topographically correlate the exact adsorption site of the C_{60} molecules with the unit cell of the oxide film at the ambient tunneling conditions. Also, the local electronic structure of the film directly underneath the molecules is indeterminate. For this, a detailed understanding of the oxide film is crucial.[13,14,26,27] The oxide consists of two alternating layers of aluminum and oxygen, with an oxygen-terminated surface roughly 5.2 Å above the NiAl(110) surface. This structure of the oxide film and its thickness may be paramount in understanding why the vibronic features can be detected in the dI/dV spectra on top of the layer. A better understanding of the spectra would require further experimentation on this and similarly prepared systems along with detailed calculations taking into account the electronic structure of the C_{60} molecules and their interaction with the NiAl(110) substrate and each other, as well as the alumina film.

Conclusion

We have shown an extension of the STM in detecting the vibronic states of single molecules on ultrathin Al_2O_3 films, thus offering the feasibility of vibrational spectroscopy on poorly conducting surfaces. A comparison of vibronic spectra of the fullerene molecules adsorbed on the alumina film at two different temperatures is presented. These spectra differ qualitatively and bear vibronic progressions whose symmetry is a function of the molecular adsorption geometry. In the case of isolated molecules, the spectra fall into two major groups, while the molecules in the monolayer have distinct spectra for each of the three orientations. In some cases, the dI/dV spectra exhibit a "progression of progressions". These experiments suggest a way toward probing local electron−phonon coupling in adsorbates. Such sensitivity to local adsorbate characteristics may be used in the exploration of novel molecular properties and their applications.

Acknowledgment. This work was supported by the Air Force Office of Scientific Research Grant No. FA9550-04-1-0181. We are grateful to C. Silien, G. V. Nazin, X. H. Qiu, X. Chen, and S. Wu for many helpful comments and suggestions.

References and Notes

(1) Nitzan, A. *Annu. Rev. Phys. Chem.* **2001**, *52*, 681.

(2) Nitzan, A.; Ratner, M. A. *Science* **2000**, *300*, 541.

(3) Heath, J. R.; Ratner, M. A. *Phys. Today* **2003**, *56*, 43.

(4) Seideman. T. *J. Phys.: Condens. Matter* **2003**, *15*, R521−R549.

(5) Haddon, R. C. *Acc. Chem. Res.* **1992**, *25*, 127.

(6) Dresselhaus, M. S.; Dresselhaus, G.; Eklund, P. C. In *Science of Fullerenes and Carbon Nanotubes*; Academic Press: San Diego, CA, 1996.

(7) Park, H.; Park, J.; Lim, A. K. L.; Anderson, E. H.; Alivisatos, A. P.; McEuen, P. L. *Nature* **2000**, *407*, 57.

(8) Park, J. W.; Pasupathy, A.; Goldsmith, J.; Soldatov, A.; Chang, C.; Yaish, Y.; Sethna, J.; Abruña, H.; Ralph, D. C.; McEuen, P. L. *Thin Solid Films* **2003**, *438*, 457.

(9) Ho, W. *J. Chem. Phys.* **2002**, *117*, 11033.

(10) Stipe, B. C.; Rezaei, M. A.; Ho, W. *Science* **1998**, *280*, 1732.

(11) Liu, N.; Pradhan, N. A.; Ho, W. *J. Chem. Phys.* **2004**, *120*, 11371.

(12) Stipe, B. C.; Rezaei, M. A.; Ho, W. *Rev. Sci. Instrum.* **1999**, *70*, 137.

(13) Stierle, A.; Renner, F.; Streitel, R.; Dosch, H.; Drube, W.; Cowie, B. C. *Science* **2004** *303*, 1652 and references therein.

(14) Kulawik, M.; Nilius, N.; Rust, H.-P.; Freund, H.-J. *Phys. Rev. Lett.* **2003**, *91*, 256101.

(15) Nilius, N.; Wallis, T. M.; Ho, W. *Phys. Rev. Lett.* **2003**, *90*, 046808.

(16) Qiu, X. H.; Nazin, G. V.; Ho, W. *Phys. Rev. Lett.* **2004**, *92*, 206102.

(17) These three orientations are not equally likely. An average over 780 molecules from seven data sets acquired in different experimental runs reveals a slight preponderance of the two-lobed orientation (40%), compared to the round and thee-lobed orientations (30% each). Each species tends to occur in small irregularly shaped groups of 10−15 molecules, without any well-defined phase boundary. No correlation between the molecular orientation and the underlying features (e.g., domain boundaries) was observed, although the effects of the substrate cannot be completely ruled out in the nucleation of these islands.

(18) For dosing at room temperature in the experiments described here, the average island size consists of 500−1000 molecules. The spectra are independent of the island size if they are measured over molecules that are not lying on the island boundaries or on top of the oxide domain boundaries. All the data presented here are for molecules adsorbed on the oxide terraces and in the island interior.

(19) Stafstrom, S. *Int. J. Mod. Phys. B* **1992**, *6*, 3853.

(20) Kondo, H.; Momose, T.; Shida, T. *Chem. Phys. Lett.* **1995**, *237*, 111.

(21) Gasyna, Z.; Andrews, L.; Schatz, P. *J. Phys. Chem.* **1992**, *96*, 1525.

(22) Estimates of the Jahn−Teller splitting of the t_{1u} level vary widely, although ref 21 reports an actual measurement of this splitting. The level splitting in our case is expected to be near the lower bound because of the minimal distortion of the molecule and the transient nature of the anion.

(23) Herzberg, G. In *Spectra of Polyatomic Molecules*; Van Nostrand & Reinhold Company: New York, 1966.

(24) Pascual, J. I.; Gómez-Herrero, J.; Sánchez-Portal, D.; Rust, H.-P. *J. Chem. Phys.* **2002**, *117*, 9531.

(25) This includes broadening due to the temperature, modulation, oscillatory degrees of freedom, and interactions with the substrate. See: Lauhon, L. J.; Ho, W. *Rev. Sci. Instrum.* **2001**, *72*, 216.

(26) Jaeger, R. M.; Kuhlenbeck, H.; Freund, H.-J.; Wuttig, M.; Hoffmann, W.; Franchy, R.; Ibach, H. *Surf. Sci.* **1991**, *259*, 235.

(27) Ceballos, G.; Song, Z.; Pascual, J. I.; Rust, H.-P.; Conrad, H.; Bäumer, M.; Freund, H.-J. *Chem. Phys. Lett.* **2002**, *359*, 41.